REVISTA INTERDISCIPLINAR DE PESQUISA EM ENGENHARIA

CILAMCE 2016
XXXVII IBERIAN LATIN AMERICAN CONGRESS ON COMPUTATIONAL METHODS IN ENGINEERING
BRASÍLIA - DF - BRAZIL

MULTI-OBJECTIVE OPTIMIZATION OF A VEHICLE'S DYNAMIC RESPONSE TO EXCITATIONS CAUSED BY A ROAD PROFILE THROUGH A META-HEURISTIC ALGORITHM

Giovani G. Fossati

Letícia F. F. Miguel

giovani.fossati@ufrgs.br

letffm@ufrgs.br

PROMEC, Universidade Federal do Rio Grande do Sul

Rua Sarmento Leite, 425, 90.050-170, Porto Alegre, RS, Brasil

Abstract. *The proposed work uses a meta-heuristic algorithm with a multi-objective approach to optimize the suspension parameters of a half car ride model, representing a passenger car, when it travels at a constant speed on a certain road profile. The numerical-computational routine developed seeks to simulate the dynamic behavior of the vehicle model in response to the excitations caused by the pavement's irregularities, and to obtain the parameters that minimize both the vertical acceleration of the driver seat and the front and rear tire deflections of the model. The ISO 8608 (1995) standard methodology is used to obtain the base excitation signals that represent the track's irregularities. The method proposed by Shinozuka and Jan (1972) is used to obtain the road irregularity profile in the time domain from the power spectral density (PSD) equations that represent the different pavement classes. The Newmark's method (1959) is used to solve the differential motion equation in order to obtain the vehicle model's responses to these irregularities. Finally, the NSGA-II meta-heuristic algorithm proposed by Deb et al. (2002) is used to obtain the optimal suspension parameters, which minimize the vertical accelerations of the driver seat.*

Keywords: *Multi-objective optimization, Half car ride model, Random road profile, PSD, NSGA-II.*

1 INTRODUCTION

The use of meta-heuristic algorithms has been increasing in mechanical systems optimization, providing speed and accuracy in obtaining an optimal result. Combining an optimization algorithm with a model that satisfactorily represents a mechanical system yields a tool that indicates the system's maximum efficiency parameters, which can be used in numerous applications.

The automotive industry faces the challenge of combining maximum safety, performance and comfort with minimum cost, weight and production time. Thus, precise numerical models of the vehicle, as well as an accurate representation of the road network, have become imperative to achieve the targeted quality standards on the manufacturing of vehicles and its components. Beyond the precision of the numerical models, many situations still require the uncovering of the best possible parameters of the vehicle's components to reach these quality standards, which can be obtained through an optimization algorithm. Ultimately, even the option between the best parameters of opposing characteristics may be demanded, which requires a multi-objective optimization algorithm (MOOA).

A vehicle suspension optimization problem is a multi-objective optimization problem (MOOP), which requires a multi-objective approach since the suspension main objectives are conflicting: to isolate the vehicle's occupants from vibrations imported from the road roughness; and to provide the vehicle a good road holding or handling by suppressing the vibration of the wheels. The first of the suspension's objectives is directly related with the occupants' comfort, which is primarily influenced by the seat motion absorbed by the driver and the passenger's bodies. Not less importantly, the suspension's second objective is mainly related to the occupants' safety, which is affected by the firmness of the tire contact with the ground.

Some of the MOOAs published in the literature have gathered high attention because of its effectiveness in obtaining a Pareto front closest to the real Pareto front when solving MOOPs. Gadhvi *et al.* (2016) compared the results of three of the most widely used multi-objective evolutionary algorithms (MOEAs) when solving a vehicle suspension MOOP. The authors concluded that marginally better optimum values are obtained with the NSGA-II algorithm.

Genetic algorithms are frequently used due to its flexibility, precision and speed, being the NSGA-II recently used by different authors to solve the vehicle suspension MOOP of different vehicle models. Shojaeefard *et al.* (2014) used the NSGA-II algorithm to perform the Pareto optimization of a five-degree of freedom vehicle vibration model travelling on a random road profile, considering three conflicting objective functions simultaneously. Nagarkar *et al.* (2016) used the same algorithm to realize a multi-objective optimization of a quarter-car and driver model travelling on a random track, given multiple comfort and stability criteria.

In this paper, the NSGA-II algorithm is used for a multi-objective optimization of a five degrees-of-freedom vehicle vibration model, travelling with a constant speed on a random road profile composed by three different pavement classes of the ISO 8608 standard (1995). The method proposed by Shinozuka and Jan (1972) is used to obtain the road irregularity profiles in the time domain from the PSD equations that represent these pavement classes. The differential motion equation of the vehicle's response to the road irregularities is solved numerically using the method proposed by Newmark (1959). Three objective functions are

considered for minimization: root mean square (RMS) values of the driver seat vertical acceleration ($\ddot{z}_c$), representing the ride comfort; RMS values of the front tire deflection ($z_{tf} - z_{Rf}$), expressing the road holding; and, similarly, RMS values of the rear tire deflection ($z_{tr} - z_{Rr}$), also expressing the road holding. The stiffness and damping coefficients of the driver seat and the front and rear suspensions form the six-variable design vector, $\vec{x}$.

2 ROAD ROUGHNESS SIMULATION

2.1 Representation of different road profiles

The road surface representation is a topic of constant investigation by several authors throughout the years. Dodds and Robson (1973) showed that a single direct PSD function provides a road surface description that is sufficient for multi-track vehicle response analysis, proposing a road classification method based on this function. Honda *et al.* (1982) developed a model for the representation of road surface roughness on highway bridges using PSD functions. The progress of the vehicle modelling studies lead to the necessity of a standard model of road roughness representation, which was consolidated by the International Organization for Standardization, through the ISO 8608 (1995) standard.

Being the only input of the passive suspension system, the road profile has a major role on the vehicle's vibration; therefore, this standard model of representation represents a great improvement on vehicle dynamics analysis. In the ISO 8608 (1995) standard, the road surface was modeled as a one variable stochastic process with an indicated PSD function. According to this standard, there is a logarithmic linear relation between the vertical displacement PSD and the spatial frequency of a given road profile. Thus, a classification system composed by different roughness pavements, illustrated in Fig. 1, could be determined.

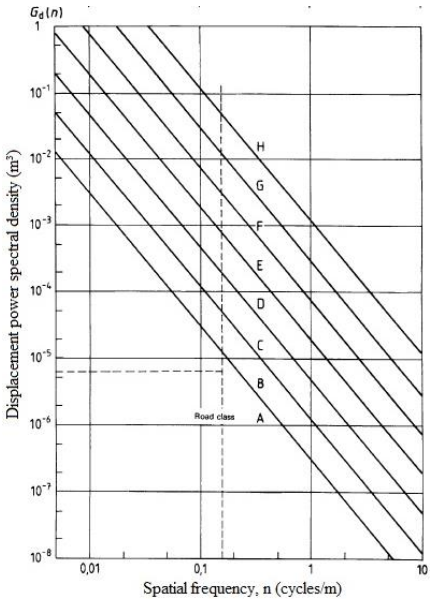

Figure 1. Road roughness classification system in terms of displacement PSDs
Source: ISO 8608 (1995)

The relation between the vertical displacement PSD and the spatial frequency is defined as:

$$G_d(n) = G_d(n_0).\left(\frac{n}{n_0}\right)^{-w} \tag{1}$$

where n_0 denotes the reference spatial frequency (cycles/m), n is the spatial frequency (cycles/m), w is the wavelength distribution, $G_d(n_0)$ is the reference vertical displacement PSD (m^3) and $G_d(n)$ is the vertical displacement PSD (m^3). The reference spatial frequency, n_0, is defined by the standard as a constant (0.1 cycle/m), and the value for the wavelength distribution, w, is usually defined as 2, which yields a constant speed PSD, meaning that the vehicle is moving at a fixed speed. The range of the spatial frequency defined by the standard goes from 0.011 cycle/m to 2.83 cycles/m. Table 1 shows the reference PSD, $G_d(n_0)$, for different classes of roads, which can provide an estimate of the degree of roughness of the road.

Table 1. Degree of roughness of different classes of roads in terms of the reference PSD

Road Class	Degree of roughness $G_d(n_0)$[(1)] (10^{-6} m^3)		
	Lower limit	Geometric mean	Upper limit
A	-	16	32
B	32	64	128
C	128	256	512
D	2048	1024	2048
E	2048	4096	8192
F	8192	16384	32768
G	32768	65536	131072
H	131072	262144	-

(1) n_0 = 0.1 cycle/m

Source: ISO 8608 (1995)

According to Reza-Kashizadeh *et al.* (2014), the displacement PSDs, in terms of spatial and time frequencies, are related according to:

$$G_d(f) = \frac{G_d(n)}{v} \tag{2}$$

where $G_d(f)$ denotes the vertical displacement PSD (m^2s) in terms of temporal frequency, $G_d(n)$ denotes the vertical displacement PSD (m^3) in terms of spatial frequency, and v is the vehicle speed (m/s).

2.2 Road profiles in the time domain

The method proposed by Shinozuka and Jan (1972) was used to obtain the road displacement signals in the time domain, which are the input parameter that represents the excitations imposed by the pavement to the suspension of the vehicle model. In this method, a PSD is used for the digital simulation of random processes, through the following equation:

$$\vec{y}(t) = \sum_{k=1}^{N} \sqrt{2G_d(f_k)\Delta f_k}\cos(2\pi f_k t + \psi_k) \tag{3}$$

where $\vec{y}(t)$ denotes temporal displacement signal of the track (m), N is the number of intervals of the frequency domain, ψ_k is an independent random phase angle (rad) uniformly distributed between 0 and 2π, and $\Delta f_k = f_{k+1} - f_k$ is the frequency variation range (Hz).

3 PASSIVE HALF-VEHICLE MODEL

A five degrees-of-freedom half-vehicle model with a passive suspension, intended to study the vertical motions and pitch of a passenger vehicle travelling on a straight line, is shown in Fig. 2. The car body is represented by the sprung mass, m_s, connected to both of the unsprung masses, m_{tf} and m_{tr}, denoting the front and rear wheel masses, respectively. The sprung mass is assumed rigid, and has freedom of motion in the vertical and in the pitch direction, while the unsprung masses are free to bounce vertically with respect to the sprung mass. A third unsprung mass, m_c, representing the seat and the driver, connects to the sprung mass and is also free to bounce vertically. The distances between the center of gravity of the sprung mass and the points where the unsprung masses connect to it are a, r and b, for the front wheel, the driver seat and the rear wheel, respectively.

The motion variables vector is composed by the five degrees-of-freedom of the half-vehicle model, z_c, z_s, θ_s, z_{tf} and z_{tr}, namely the seat and the sprung mass vertical displacements, the pitch angle, and the front and rear wheel vertical displacements, respectively. The pitch angle, θ_s, is assumed to be small. The vertical displacement imposed to the vehicle model by the road irregularities is represented by z_{Rf}, for the front wheel, and z_{Rr}, for the rear wheel. The front and rear stiffness coefficients are given by k_f and k_r for the suspension and k_{tf} and k_{tr} for the tires, respectively. Similarly, the front and rear damping coefficients are given by c_f and c_r for the suspension and c_{tf} and c_{tr} for the tires, respectively. The seat stiffness and damping coefficients are denoted by k_s and c_s, respectively.

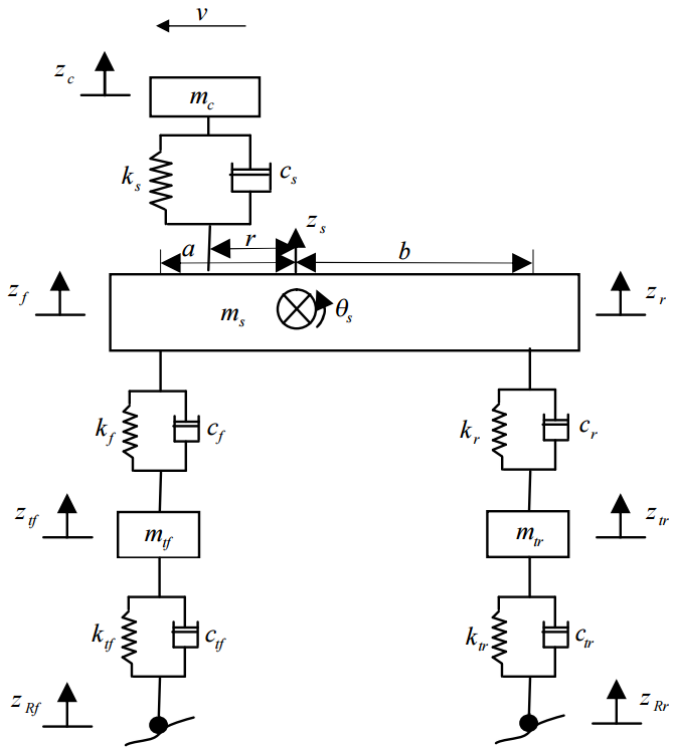

Figure 2. Five degrees-of-freedom passive half-vehicle model
Source: Adapted from Shojaeefard *et al.* (2014)

The linearized differential equations of motion, with respect to the five degrees-of-freedom of the model, can be written as follows:

$$m_c\ddot{z}_c = -k_s(z_c - z_s - r\theta_s) - c_s(\dot{z}_c - \dot{z}_s - r\dot{\theta}_s) \tag{4}$$

$$m_s\ddot{z}_s = k_s(z_c - z_s - r\theta_s) + c_s(\dot{z}_c - \dot{z}_s - r\dot{\theta}_s) \tag{5}$$

$$I_s\ddot{\theta}_s = r\left[k_s(z_c - z_s - r\theta_s) + c_s(\dot{z}_c - \dot{z}_s - r\dot{\theta}_s)\right] \tag{6}$$

$$m_{tf}\ddot{z}_{tf} = -k_{tf}(z_{tf} - z_{Rf}) - c_{tf}(\dot{z}_{tf} - \dot{z}_{Rf}) \tag{7}$$

$$m_{tr}\ddot{z}_{tr} = -k_{tr}(z_{tr} - z_{Rr}) - c_{tr}(\dot{z}_{tr} - \dot{z}_{Rr}) \tag{8}$$

The motion equations are a set of five, second order ordinary differential equations, and can be written in the matrix form as shown in Eq. (9). The implicit numerical integration method proposed by Newmark (1959) was used for the dynamic analysis of the proposed model.

$$[M]\vec{\ddot{z}}(t) + [C]\vec{\dot{z}}(t) + [K]\vec{z}(t) = \vec{F}(t) \tag{9}$$

where $[M]$, $[C]$ and $[K]$ are the mass, damping and stiffness matrices, respectively, $\vec{F}(t)$ is the forcing function vector, and $\vec{z}(t)$ is the motion variables vector. These matrices and vectors are displayed below, considering the half-vehicle model in study:

$$[M] = \begin{bmatrix} m_c & 0 & 0 & 0 & 0 \\ 0 & m_s & 0 & 0 & 0 \\ 0 & 0 & I_s & 0 & 0 \\ 0 & 0 & 0 & m_{tf} & 0 \\ 0 & 0 & 0 & 0 & m_{tr} \end{bmatrix} \tag{10}$$

$$[C] = \begin{bmatrix} c_s & -c_s & rc_s & 0 & 0 \\ -c_s & c_s + c_f + c_r & -rc_s - ac_f + bc_r & -c_f & -c_r \\ rc_s & -rc_s - ac_f + bc_r & r^2c_s + a^2c_f + b^2c_r & ac_f & -bc_r \\ 0 & -c_f & ac_f & c_f + c_{tf} & 0 \\ 0 & -c_r & -bc_r & 0 & c_r + c_{tr} \end{bmatrix} \tag{11}$$

$$[K] = \begin{bmatrix} k_s & -k_s & rk_s & 0 & 0 \\ -k_s & k_s + k_f + k_r & -rk_s - ak_f + bk_r & -k_f & -k_r \\ rk_s & -rk_s - ak_f + bk_r & r^2k_s + a^2k_f + b^2k_r & ak_f & -bk_r \\ 0 & -k_f & ak_f & k_f + k_{tf} & 0 \\ 0 & -k_r & -bk_r & 0 & k_r + k_{tr} \end{bmatrix} \tag{12}$$

$$\vec{F} = \begin{bmatrix} 0 & 0 & 0 & k_{tf}z_{Rf} + c_{tf}\dot{z}_{Rf} & k_{tr}z_{Rr} + c_{tr}\dot{z}_{Rr} \end{bmatrix}^T \tag{13}$$

$$\vec{z}(t) = \begin{bmatrix} z_c & z_s & \theta_s & z_{tf} & z_{tr} \end{bmatrix}^T \tag{14}$$

4 MULTI-OBJECTIVE OPTIMIZATION OF THE VEHICLE MODEL

4.1 Multi-objective optimization

An optimization process that simultaneously finds the best possible set of solutions for two or more conflicting objectives, subject to certain constraints, is defined as multi-objective optimization. Mathematically, a MOOP can be written as:

$$\min \vec{F}(\vec{x}) = [f_1(\vec{x}), f_2(\vec{x}), \dots, f_k(\vec{x})]^T \tag{15}$$

subject to

$$g_i(\vec{x}) \leq 0\,, i = 1, 2, \dots, p \tag{16}$$

$$h_j(\vec{x}) = 0\,, j = 1, 2, \dots, q \tag{17}$$

$$x_{i,lb} \leq x_i \leq x_{i,ub}\,, i = 1,2, \dots, n \tag{18}$$

where $\vec{x} = [x_1,\ x_2, \dots, x_n] \in \mathbb{R}^n$ is the design variables vector, $\vec{F}(\vec{x}) \in \mathbb{R}^k$ is the vector of objective functions, $g_i(\vec{x})$ are the inequality constraints, $h_j(\vec{x})$ are the equality constraints, $x_{i,lb}$ are the design variables lower bounds, and $x_{i,ub}$ are the design variables upper bounds.

The solution of a MOOP provides a Pareto optimal front, composed by multiple optimal solutions. The non-dominated optimized points that form the Pareto set offer a range of best possible solutions for a given problem, so the chosen optimal point can be the one that best suits the designing conditions of that problem. A MOOP may also be a maximization problem, which, mathematically, is equivalent to a minimization problem of the objective function's negative values.

4.2 The NSGA-II Algorithm

A genetic algorithm (GA) is a meta-heuristic algorithm based on the evolutionary principles of natural selection. According to Goldberg *et al.* (1989) and Haftka *et al.* (1993), the optimization GA starts from an initial set, or first generation, of randomly chosen designs with uniform probability distribution. Given a current generation of designs, the algorithm is implemented in three steps: reproduction, crossover and mutation. The population size maintains the same throughout the optimization steps, and a complete iteration or new generation of designs is formed after completing all three steps. This process is then repeated for the new generation.

In the non-dominated sorting genetic algorithm (NSGA-II), each solution, or individual, is compared to the remaining individuals of a population, and then all non-dominated solutions and non-dominated fronts are identified and ranked with different fitness values. After the sorting, the crowding distance parameter is assigned to each individual, and measures the proximity to its neighbors. Parents are selected from de non-dominated front, and new offsprings are created using mutation and crossover operators. The new generation of offsprings is then combined with the current population to generate a new one, and the selection is proceeded on the next generation individuals (Deb *et al.*, 2002).

The flexibility, precision and speed of the NSGA-II algorithm was compared to other consolidated and widely used MOOAs in a recent study performed by Gadhvi *et al.* (2016), which compared multi-objective optimization solutions of a vehicle model's suspension system. The authors compared the results of three of the most widely used multi-objective evolutionary algorithms (MOEAs) when solving a vehicle suspension MOOP: the elitist based non-dominated sorting genetic algorithm (NSGA-II) by Deb *et al.* (2002); strength Pareto evolutionary algorithm (SPEA2) by Zitzler *et al.* (2001); and region based Pareto Envelope based Selection Algorithm (PESA-II), by Corne *et al.* (2001). It was shown that the Pareto fronts obtained from NSGA-II yielded extreme trade-off optimal points giving marginally better optimum values of the objective vector as compared to SPEA2 and PESA-II, with a

slightly less diversified Pareto front. In the present study, the importance of obtaining better optimal results was favored instead of a more diversified set of optimal solutions, besides the fact that the NSGA-II algorithm has also presented a satisfactory diversification of the Pareto front, justifying the choice of this algorithm.

4.3 Multi-objective Optimization of a passive half-vehicle model

For a multi-objective optimization of a vehicle suspension system, the objective functions needs to be composed of parameters that represent the performance of this system. According to Baumal *et al.* (1998), there are three characteristics commonly used to assess the performance of vehicle suspension systems: *ride comfort*, which improves as the magnitude of the seat acceleration, $|\ddot{z}_c|$, decreases; *road-holding ability or safety*, which is acceptable for restricted or low tire-road contact forces and is quantified by the front tire deflection, $(z_{tf} - z_{Rf})$, or the rear tire deflection, $(z_{tr} - z_{Rr})$; and the *suspension working space*, which must be restricted and is given by $(z_s - a\theta_s - z_{tf})$ for the front wheel and by $(z_s + b\theta_s - z_{tr})$ for the rear wheel. In the present study, the root mean square (RMS) values of the first two characteristics are defined as the objective functions to minimize, resulting in three objective functions, $f_1(x)$, $f_2(x)$ and $f_3(x)$, to be optimized simultaneously.

The design variables vector, composed by the remaining six unknown parameters of the vehicle model, is given by Eq. (19). The constant parameters of the model, adopted according to Haug *et al.* (1979) and converted to SI units, are presented in the Table 2.

$$\vec{x} = \begin{bmatrix} k_s & c_s & k_f & c_f & k_r & c_r \end{bmatrix}^T \tag{19}$$

Table 2. Fixed parameters of the half-vehicle model

Parameter	Nomenclature	Value	Unit
Seat and driver mass	m_c	132	kg
Sprung mass	m_s	2040	kg
Pitch moment of inertia	I_s	4630	kg.m^2
Front wheel mass	m_{tf}	44	kg
Rear wheel mass	m_{tr}	44	kg
Front tire stiffness coefficient	k_{tf}	262700	N/m
Rear tire stiffness coefficient	k_{tr}	262700	N/m
Front tire damping coefficient	c_{tf}	876	N.s/m
Rear tire damping coefficient	c_{tr}	876	N.s/m
Longitudinal distance between the seat and the sprung mass c.g.	a	1.01	m
Longitudinal distance between the front axle c.g. to the sprung mass c.g.	b	2.03	m
Longitudinal distance between the rear axle c.g. to the sprung mass c.g.	r	0.25	m

The half-vehicle model is supposed to travel at a constant speed of 24.4 m/s over a road profile composed by classes A, B and C of the ISO 8608 standard, portrayed in the Fig. 3 for the front and rear wheels of the model. The lag time between wheels is given by Eq. (20).

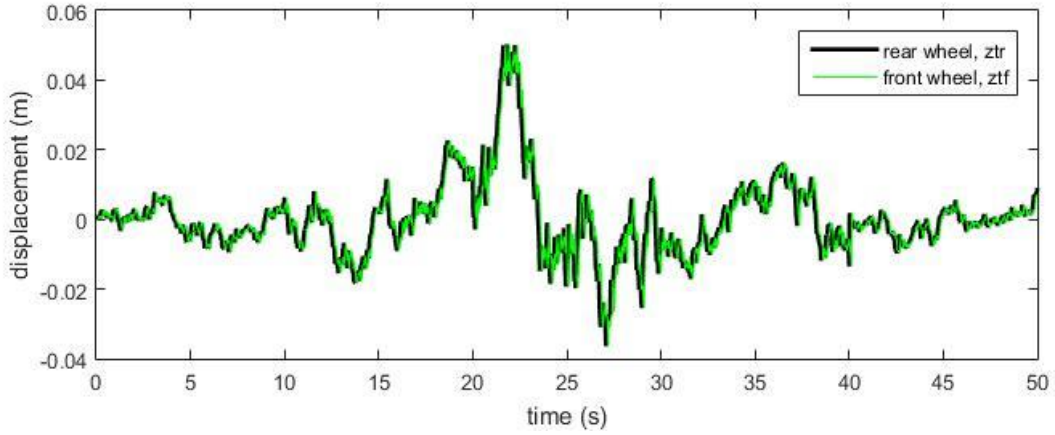

Figure 3. Road profile composed by classes A, B and C of the ISO 8608 standard

$$\tau = \frac{a+b}{v} \tag{20}$$

The optimization problem presented in this paper is a modified version of the single objective optimization problem described by Baumal *et al.* (1998), and can be written as:

$$\min \vec{F}(\vec{x}) = [f_1(\vec{x}) \quad f_2(\vec{x}) \quad f_3(\vec{x})]^T \tag{21}$$

where

$$f_1(\vec{x}) = \sqrt{\frac{1}{T}\int_0^T \ddot{z}_c^2 dt} \tag{22}$$

$$f_2(\vec{x}) = \sqrt{\frac{1}{T}\int_0^T \left(z_{tf} - z_{Rf}\right)^2 dt} \tag{23}$$

$$f_3(\vec{x}) = \sqrt{\frac{1}{T}\int_0^T (z_{tr} - z_{Rr})^2 dt} \tag{24}$$

subject to

$$8756\ N/m \leq x_1 \leq 87563\ N/m \quad (25)$$

$$350\ N.s/m \leq x_2 \leq 8756\ N.s/m \quad (26)$$

$$35025\ N/m \leq x_3 \leq 175127\ N/m \quad (27)$$

$$875\ N.s/m \leq x_4 \leq 14010\ N.s/m \quad (28)$$

$$35025\ N/m \leq x_5 \leq 175127\ N/m \quad (29)$$

$$875\ N.s/m \leq x_6 \leq 14010\ N.s/m \quad (30)$$

where Eq. (21) denotes the vector of objective functions to minimize; Eqs. (22) through (24) explicit the objective functions, namely, the RMS values of the seat acceleration and the front and rear tire deflection signals, respectively; and Eqs. (25) through (30) determine the lower and upper bounds that limit the design variables within a certain range.

5 RESULTS AND DISCUSSION

The proposed MOOP was solved using the NSGA-II algorithm, using a population of 200 individuals with a crossover probability of 0.9 and a mutation probability of 0.1. These criteria were used in 3000 generations. Figure 4 shows the results of the three objective optimization in the $f_1(\vec{x})$ - $f_2(\vec{x})$ plane, as well as the extreme trade-off points for this plane, denoted by A and B. Similarly, Fig. 5 shows the results of the three objective optimization in the $f_1(\vec{x})$ - $f_3(\vec{x})$ plane, as well as the extreme trade-off points for this plane.

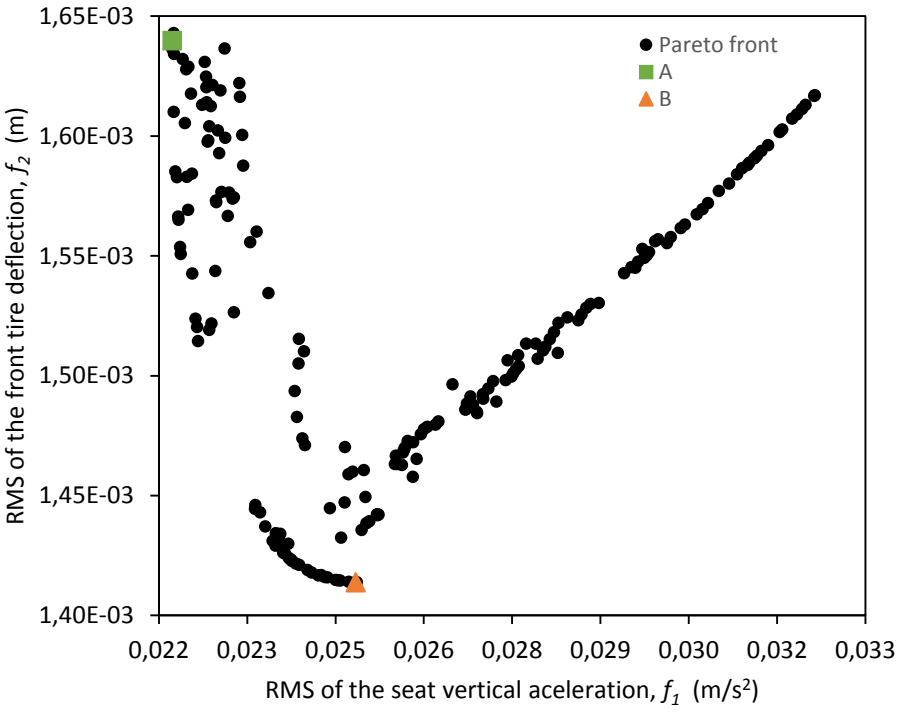

Figure 4. Pareto front and extreme trade-off points of the $f_1(\vec{x})$ - $f_2(\vec{x})$ plane obtained using the NSGA-II algorithm

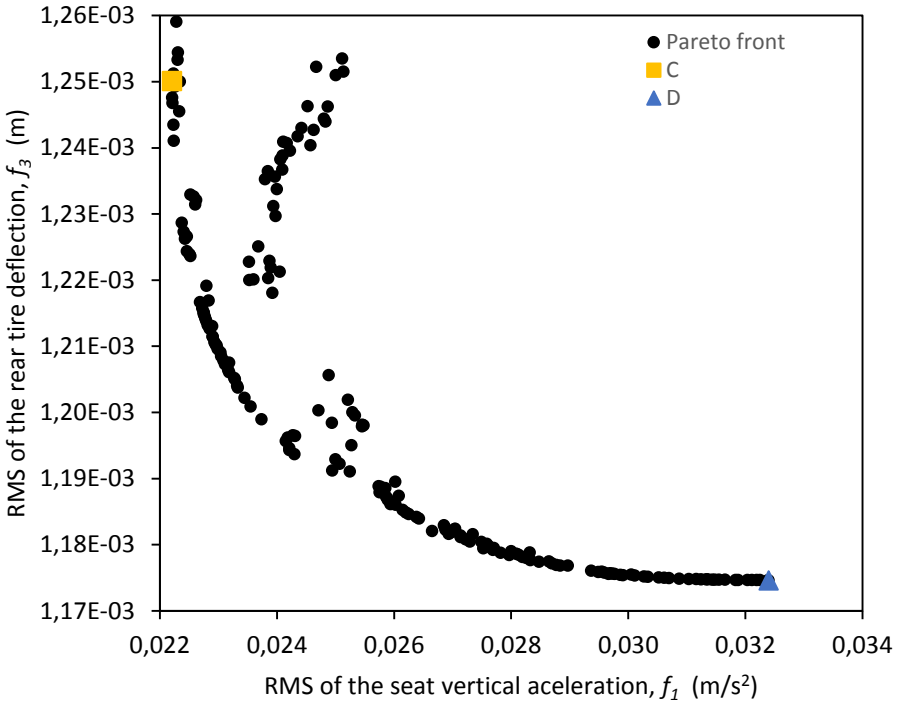

Figure 5. Pareto front and extreme trade-off points of the $f_1(\vec{x})$ - $f_3(\vec{x})$ plane obtained using the NSGA-II algorithm

As can be seen in Figs. 4 and 5, the $f_1(\vec{x})$ - $f_2(\vec{x})$ plane has a wider spread of optimal solutions when compared to the $f_1(\vec{x})$ - $f_3(\vec{x})$ plane. This means that the spread of the front tire deflection is approximately 2.5 times wider than the rear tire deflection, for virtually the same range of variation of the seat acceleration, in terms of objective functions. The $f_2(\vec{x})$ - $f_3(\vec{x})$ plane is not presented in this study because, according to Gadhvi *et al.* (2016), the Pareto front of this plane is not important to make a decision regarding optimized design parameters of individual suspensions.

The three objective optimization results and the extreme trade-off points in the $f_1(\vec{x})$ - $f_2(\vec{x})$ - $f_3(\vec{x})$ space are displayed in Fig. 6. This figure shows that the extreme points A and C, which respectively minimizes the seat vertical acceleration in the $f_1(\vec{x})$ - $f_2(\vec{x})$ and $f_1(\vec{x})$ - $f_3(\vec{x})$ planes, are coincident.

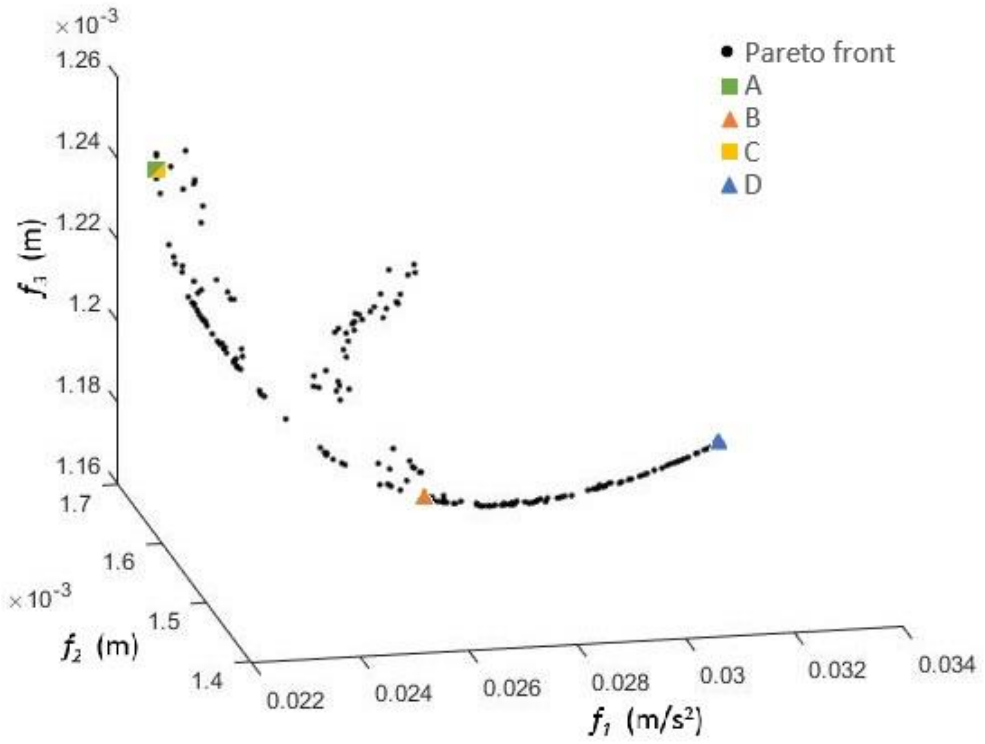

Figure 6. Pareto front and extreme trade-off points of the $f_1(\vec{x})$ - $f_2(\vec{x})$ - $f_3(\vec{x})$ space obtained using the NSGA-II algorithm

The three-dimensional Pareto front presented displays a generation of 200 optimized solutions of the problem, including the extreme points that represent the sets of design variables that minimize each of the objective functions individually. The Table 3 presents the values of the design variables and objective functions in these extreme points. This front represents a decision-making tool that aids in the choosing of the optimal set of design variables that best suits the solution of the real problem.

Table 3. Values of the design variables and objective functions in the extreme trade-off points obtained

Design Point	k_s (N/m)	c_s (N.s/m)	k_f (N/m)	c_f (N.s/m)	k_r (N/m)	c_r (N.s/m)	f_1 (m/s²)	f_2 (m)	f_3 (m)
A	40477.62	350.00	50285.53	3849.29	35025.00	1169.51	0.02221	0.00164	0.00125
B	40521.98	2497.55	50154.66	1915.35	35025.00	875.00	0.02512	0.00141	0.00125
C	40477.62	350.00	50285.53	3849.29	35025.00	1169.51	0.02221	0.00164	0.00125
D	40476.62	6250.94	50732.73	875.00	35025.00	1838.14	0.03240	0.00162	0.00117

The dynamic response of the half-vehicle model to the proposed road profile, using the set of design variables from the extreme point A or C, which minimizes the RMS value of the seat vertical acceleration, $f_1(\vec{x})$, is portrayed on Fig. 7. This figure displays the temporal signals of the motion variables vector, $\vec{z}(t)$, as well as its first and second derivatives, $\dot{\vec{z}}(t)$ and $\ddot{\vec{z}}(t)$, in response to the excitations caused by the proposed road profile. These vectors represent the vertical displacement, velocity and acceleration of the half vehicle model's motion variables.

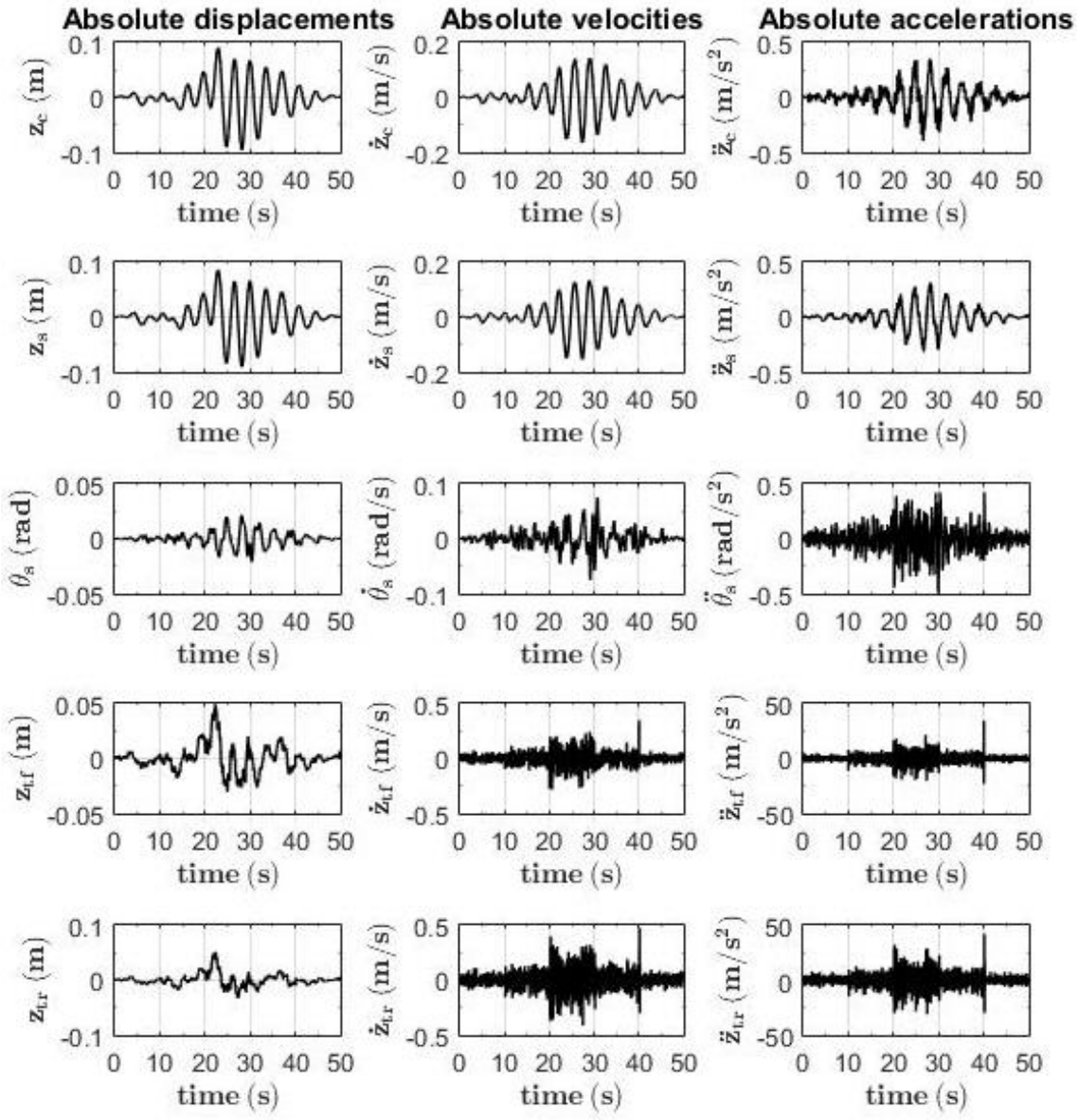

Figure 7. Displacements, velocities and accelerations of the half-vehicle model's motion variables, using parameters that minimize the RMS value of the seat vertical acceleration, $f_1(\vec{x})$

The temporal signals used to obtain the RMS values of the three objective functions, $f_1(\vec{x})$, $f_2(\vec{x})$ and $f_3(\vec{x})$, using the set of design variables from the extreme point A or C, which minimizes the RMS value of the seat vertical acceleration, $f_1(\vec{x})$, are displayed in Fig. 8. These signals represent the seat vertical acceleration, $\ddot{z}_c(t)$, the front tire deflection, $(z_{tf} - z_{Rf})$, and the rear tire deflection, $(z_{tr} - z_{Rr})$, respectively.

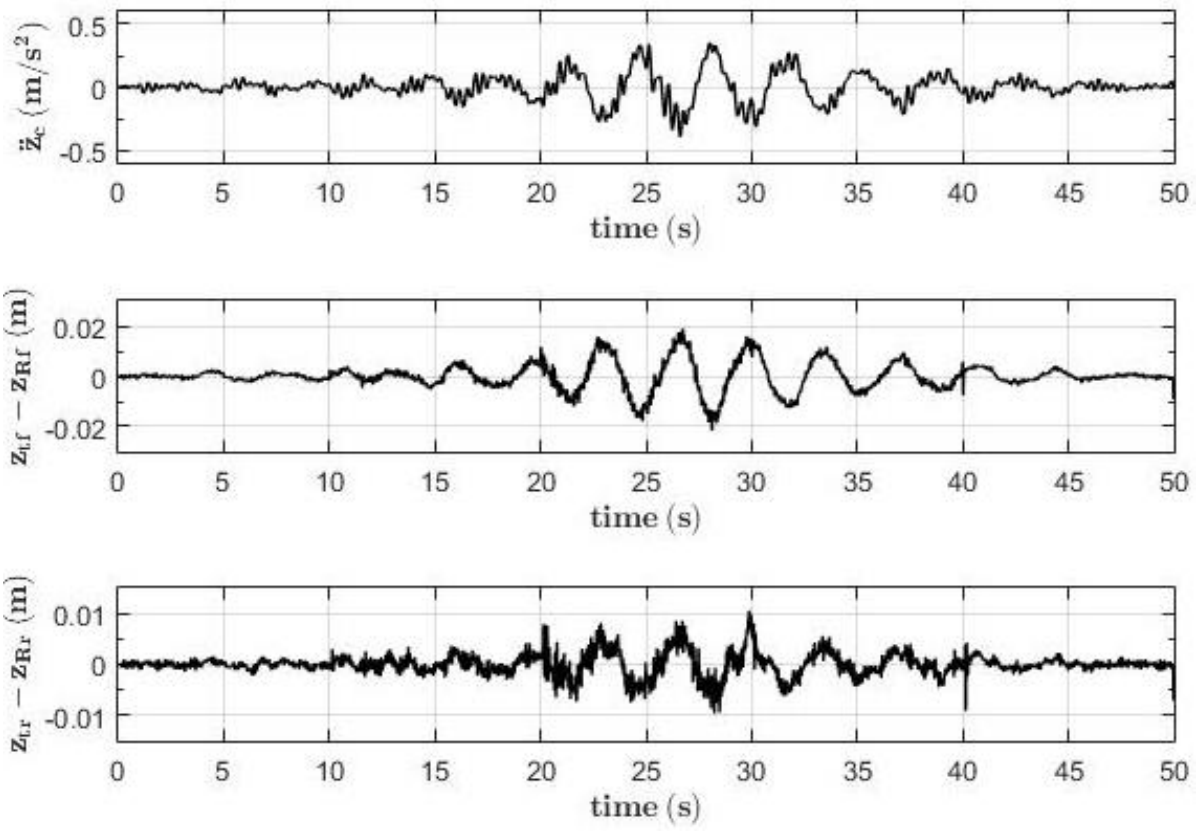

Figure 8. Seat vertical acceleration, $\ddot{z}_c(t)$, front tire deflection, $(z_{tf} - z_{Rf})$, and rear tire deflection, $(z_{tr} - z_{Rr})$ of the half-vehicle model's motion variables, using parameters that minimize the RMS value of the seat vertical acceleration, $f_1(\vec{x})$

6 CONCLUSIONS

This paper presented a methodology to improve the design of a vehicle's suspension system. The modified non-dominated sorting genetic algorithm (NSGA-II) was used to solve the multi-objective optimization problem of the passive suspension system of a half-vehicle model travelling on a random road profile. The road roughness was modeled as a composition of random processes with determined PSDs specified in the ISO 8608 Standard.

The optimization process considered three objective functions that represented conflicting objectives – comfort and safety of the vehicle model. The process resulted in the obtainment of a three-objective Pareto front, in which the extreme trade-off design sets were compared and further studied. The Pareto front has proven to be an effective way of providing a variety of optimal design sets, which assist the designer in the decision of choosing the one that best suits the solution of the real problem. The use of random road profiles to conduct the study elevates the computational cost, but yields more realistic design variables than using a less sophisticated excitation road profile.

ACKNOWLEDGEMENTS

The authors acknowledge the CAPES and the CNPq financial support to this research.

REFERENCES

Baumal, A. E., McPhee, J. J., & Calamai, P. H., 1998. Application of genetic algorithms to the design optimization of an active vehicle suspension system. *Computer Methods in Applied Mechanics and Engineering*, vol. 163, pp. 87 – 94.

Corne, D. W., Jerram, N. R., Knowles, J.D., et al., 2001. PESA-II: Region-based selection in evolutionary multiobjective optimization. *Proceedings of the Genetic and Evolutionary Computation Conference (GECCO'2001*), pp. 283 - 290.

Deb, K., Pratap, A., Agarwal, S., et al., 2002. A fast and elitist multiobjective genetic algorithm: NSGA-II. *Evolutionary Computation, IEEE Transactions*, vol. 6, pp. 182-197.

Gadhvi, B., Savsani, V., & Patel, V., 2016. Multi-Objective Optimization of Vehicle Passive Suspension System using NSGA-II, SPEA2 and PESA-II. *Procedia Technology*, vol. 23, pp. 361–368.

Goldberg, D. E., 1989. *Genetic Algorithms in Search, Optimization and Machine Learning*. Addison-Wesley.

Haftka, R. T., & Gürdal, Z., 1993. *Elements of Structural Optimization.* Kluwer Academic Publishers.

Haug, E. J., & Arora, J. S., 1979. *Applied Optimal Design: Mechanical and Structural Systems.* John Wiley and Sons.

International Organization for Standardization ISO 8608, 1995. *Mechanical Vibration – Road Surface Profiles – Reporting of Measured Data.* Switzerland.

Nagarkar, M. P., Patil, G. J. V., & Patil, R. N. Z., 2016. Optimization of nonlinear quarter car suspension-seat-driver model. *Journal of Advanced Research* [Epub ahead of print].

Newmark, N. M., 1959. A Method of Computation for Structural Dynamics. *ASCE Journal of Engineering Mechanics Division*, vol. 85, n. EM3.

Shinozuka, M., & Jan, C. M., 1972. Digital Simulation of Random Process and its applications. *Journal of Sound and Vibration*, vol. 25, pp. 111-118.

Shojaeefard, M. H., Khalkhali, A., & Erfani, P. S., 2014. Multiobjective suspension optimization of a 5-DOF vehicle vibration model excited by random road profile. *International Journal of Advanced Design and Manufacturing Technology*, vol. 7, n. 1, pp. 1 - 7.

Zitzler, E., Laumanns, M., Thiele, L., et al., 2001. *SPEA2: Improving the strength Pareto evolutionary algorithm*. TIK-Report 103, Institut für Technische Informatik und Kommunikationsnetze (TIK), Eidgenössische Technische Hochschule Zürich (ETH).